BUSITEMA UNIVERSITY
Pursuing Excellence

P.O. Box 236, Tororo, Uganda
Gen: +256 - 45 444 8838
Fax: +256 - 45 4436517
Email: info@adm.busitema.ac.ug

www.busitema.ac.ug

INVESTIGATING THE IMPACT OF GEOMAGNETIC STORMS ON ZENITH TOTAL DELAY

BY

MULABBI ERUKAMU

BU/UG/2021/0073

***Supervisor*: Dr. ANDIMA GEOFFREY**

A PROJECT REPORT SUBMITTED TO THE DEPARTMENT OF PHYSICS IN PARTIAL FULFILMENT FOR THE REQUIREMENT FOR THE AWARD OF BACHELOR OF SCIENCE EDUCATION OF BUSITEMA UNIVERSITY.

July, 2024

DECLARATION

I the undersigned, declare that this research report is my original work and that it has never been submitted to any institution for an academic award.

Student Name: ..MULABBI.....ERUKAM.V.....

Registration Number: ...BU/UG/2021/0073.....

Signature: .....M.....

Date .....21st October, 2024.....

APPROVAL

This research report is submitted in a partial fulfillment for the award of bachelor science education of Busitema University, with the approval of the following

Academic supervisor

Name: Dr. Andima Geoffrey

Academic Qualifications: PhD

Rank: Senior Lecturer

Department: Physics

Faculty: Science and Education

Signature: 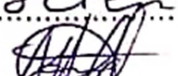

Date 21/1/2024

ACKNOWLEDGMENT

I would like to express my sincere gratitude to all the individuals who have supported and contributed to this research study.

Gratitude is extended to my supervisors, for their guidance, insightful feedback, and continuous support throughout this research. Their expertise and encouragement were valuable in shaping the direction and quality of this work.

I extent my appreciations to all my colleagues who have generously shared their time and knowledge for this study. Their contributions have been essential in the developing this research paper.

I would like to thank my family and friends for their unwavering support, encouragement and positive environment throughout this research endeavor. Their belief in me has been a constant source of motivation.

I appreciate my colleagues and peers, whose discussions and collaborative efforts enriched this study. Your solidarity and intellectual contributions were deeply appreciated.

Gratitude is also extended to the organizations and agencies that provided the data and resources crucial for this research. Their contributions made it possible to accurately identify geomagnetic storms, assess the diurnal variations in zenith total delay, and analyze the effects of these storms on ZTD.

TABLE OF CONTENTS

DECLARATION ii
APPROVAL iii
ACKNOWLEDGMENT iv
TABLE OF CONTENTS v
LIST OF FIGURES vii
LIST OF TABLES viii
List of acroym ix
CHAPTER ONE: INTRODUCTION 1
1.1 Background 1
1.2 Problem statement 2
1.3 Aim 3
1.4 Objectives 3
1.6 Scope 3
1.7 Significance 4
2.0 CHAPTER TWO: LITERATURE REVIEW 5
2.1 Space weather events. 5
2.2 Geomagnetic storms. 6
2.3 Propagation of radio signals. 6
2.3 The ZTD. 7
3.0 CHAPTER THREE: METHODS 9
3.1 Identifying Geomagnetic storms 9
3.2 Determination of diurnal variation of ZTD. 9
3.3 Determination ZTD variations during storm periods 9
4.0 CHAPTER FOUR: RESULTS AND INTERPRETATION 10
4.1 Identification of the storm. 10
4.2 Diurnal variation of ZTD 15
4.3 Variation of ZTD during storm days 19
4.4 Comparison of ZTD at the magnetic equator and the magnetic crest 22
5.0 CHAPTER 5: CONCLUSION AND RECOMMENDATION 30
5.1 Conclusion 30

5.2 Recommendations 30
References 31

LIST OF FIGURES

Figure 1.1.1: illustration of effect of fluctuation in optical density on signal propagation..... 1

Figure 2.1. 1: Solar flares 5

Figure 2.2. 1: Interaction of earth's field and space weather events 6
Figure 2.2. 2: Weakened earth's fields due to space weather events 6

Figure 4.1. 1: A severe geomagnetic storm with a minimum Dst index of $-234nT$..... 10
Figure 4.1. 2: A severe geomagnetic storm with a minimum Dst index of $-198nT$..... 12
Figure 4.1. 3: A severe geomagnetic storm with a minimum Dst index of $-166nT$..... 13

Figure 4.2. 1: Diurnal variation of ZTD for 16th March, 2015, recorded by the IGS at the magnetic equatorial region (ADIS)..... 15
Figure 4.2. 2: Diurnal variation of ZTD on 16th March, 2015, recorded by the IGS at the magnetic crest region (MAL2)..... 15
Figure 4.2. 3 Diurnal variation of ZTD on 21st June, 2015, recorded by the IGS at the magnetic equator region (ADIS)..... 16
Figure 4.2. 4: Diurnal variation of ZTD on 21st June, 2015, recorded by the IGS at the magnetic crest region (MAL2)..... 16
Figure 4.2. 5 Diurnal variation of ZTD for 19th December, 2015, recorded by the IGS at the magnetic equatorial region (ADIS)..... 17
Figure 4.2. 6: Diurnal variation of ZTD on 19th Decenber, 2015, recorded by the IGS at the magnetic crest region (MAL2)..... 17

Figure 4.3. 1: variation of ZTD during storm days in March, 2015 recorded by the reciever at the magnetic equator (ADIS)..... 19
Figure 4.3. 2: Variations of ZTD during storm days of March, 2015 as recorded by the reciever in the crest region (MAL2)..... 19
Figure 4.3. 3: Variations of ZTD during storm days of June, 2015 as recorded by the reciever at the magnetic equator (ADIS)..... 20
Figure 4.3. 4: Variations of ZTD during storm days of June, 2015 as recorded by the reciever in the magnetic crest region (MAL2)..... 21
Figure 4.3. 5: Variations of ZTD during storm days of December, 2015 as recorded by the reciever at the magnetic equator (ADIS)..... 21
Figure 4.3. 6: Variations of ZTD during storm days of December, 2015 as recorded by the reciever in the magnetic crest region (MAL2)..... 21

LIST OF TABLES

Table 4.5.1: Correlation data for average hourly ZTD value and Dst for 17th March, 2015. 23
Table 4.5.2: Correlation data for average hourly ZTD value and Dst for 23rd June, 2015. .. 25
Table 4.5.3: Correlation data for average hourly ZTD value and Dst for 17th March, 2016. 27

List of acroym

Dst	distance stom time
ZTD	zenith total delay
GNSS	Global navigation satelite system
IGS	international geomagnetic station
CME	Coronal Mass Ejection
ICME	Interplanetary Coronal Mass Ejection
TEC	total electron content
GPS	Global Positioning System

ABSTRACT

Geomagnetic storms pose a significant threat to modern communication systems and navigation technologies. They cause disturbances in the earth's magnetic fields, ionosphere, and troposphere, leading to variation in zenith total delay (ZTD), which can result into position and navigation errors. The ZTD is a critical parameter affecting Global Navigation Satellite System (GNSS) and radio communication networks.

This study investigated the impact of geomagnetic storms on zenith total delay ZTD); the research was structured around three primary objectives, That's; identifying geomagnetic storms, determining the diurnal variation of ZTD, and analyzing ZTD variations during geomagnetic storm events.

To identify geomagnetic storms, the study utilized data for the Distance storm time (Dst) index, which measures geomagnetic activity. In this study, three intense storms that occurred on March 18th, 2015, June 23rd, 2015, and December 20th, 2015 were identified with Dst index values of -234nT, -198nT, and -166nT, respectively.

The results of this study show a distinct diurnal pattern, with ZTD values peaking in the afternoon and reaching their lowest levels during the early morning hours, with peak values of around 2.5 metres in the magnetic crest regions and with peak values of 1.8 metres in the magnetic equator regions.

To assess the impact of geomagnetic storms on ZTD, the ZTD measurements during the identified storm dates were compared with the diurnal variation. The analysis of this research show that during the storms, ZTD varied up to 2.9 metres in the magnetic crest regions and up to 1.9 metres in the magnetic equator regions, with maximum deviations from quiet-day values of 0.1meter, that's ZTD increased by approximately 10% during storm periods, implying a disruption in the regular diurnal cycle. These deviations are attributed to ionospheric perturbations caused by enhanced geomagnetic activity, which increases the electron content in the ionosphere and consequently affects the delay of GPS signals.

These findings reveal that the intensity and duration of the storms increase the magnitude and duration of ZTD variations. These findings have important implications for improving the accuracy and reliability of satellite-based applications during space weather events.

Understanding these impacts is crucial for improving the reliability of communication and navigation systems during space weather events. Further research is recommended to develop predictive models that can mitigate the adverse effects of geomagnetic storms on ZTD and communication systems.

Key words: geomagnetic storms, zenith total delay, GNSS, communication systems, ionosphere, troposphere, space weather.

CHAPTER ONE: INTRODUCTION

1.1 Background

When the GNSS signals travel in the atmosphere from the satellites to the ground-based recievers on Earth, they are delayed by several processes (Bonafoni, Biondi, Brenot, & Anthes, 2019), specifically reflection and refraction processes depending on the optical density of the atmosphere, water vapour, hydrometeors (particularly the liquid content of the clouds and heavy rainfall) and other particles such as sand, dust, aerosols, and volcanic ash in the troposphere. This leads to a change in the signal's velocity, thereby affecting the GNSS positioning accuracy (Papadimitratos & Jovanovic, 2008).

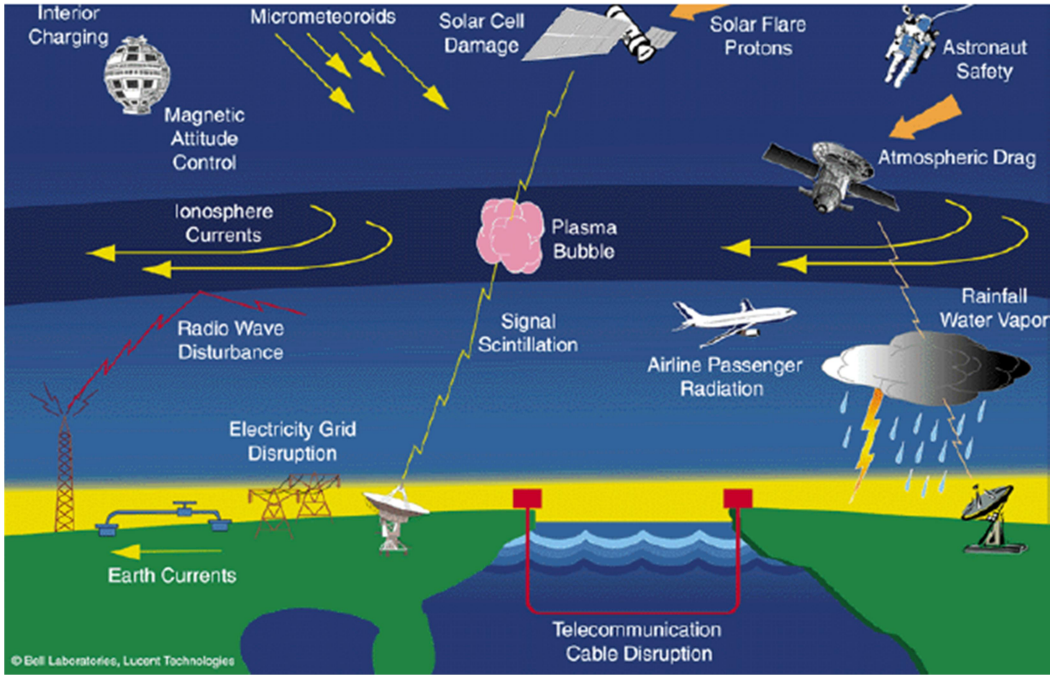

Figure 1.1.1: Illustration of effect of fluctuation in optical density on signal propagation

The delays or errors induced on GNSS signals during their propagation through the atmosphere are referred to as ionospheric and tropospheric delays (Ssenyunzi et al., 2019). Ionospheric delay is caused by the presence of free electrons in the ionosphere which is the ionized portion of the upper atmosphere. The ionospheric delay is dispersive in nature and depends on the frequency of the signal (Bhattacharyya, 2022). It can be

eliminated by the use of a linear combination of two or multiple frequencies since the GNSS broadcasts at two or more separate frequencies. Unlike the ionospheric delay, the delay due to the neutral part of the atmosphere does not depend on signal frequencies (Younes, 2018). It is mostly caused by the troposphere and is referred to as the tropospheric delay. The tropospheric delay consists of the dry or hydrostatic and wet components. The wet component which is normally the largest source of inconsistency in the atmospheric delay, depends on the content of water vapour in the troposphere (Meyer & Jin, 2016). Therefore, this study focused on the tropospheric delay since it has turned out to be a very important source of information on atmospheric water content that is a vital ingredient in meteorology applications and climate studies. The total delay path mapped onto the zenith direction is referred to as the Zenith Tropospheric (or Total) Delay (ZTD) (Bock, Willis, Lacarra, & Bosser, 2010). The ZTD refers to the delay experienced by electromagnetic signals as they pass through the Earth's atmosphere from space to the ground(Suparta, Alauddin, Ali, Yatim, & Misran, 2007). It is an essential parameter in various applications, such as GNSS, meteorology, and climate studies(Guerova et al., 2016). Accurate measurements of ZTD are crucial for precise positioning, and communication systems.

The sun is continuous emitting huge amount of energy and charged particles into the space(Horányi, 1996). When the sun suddenly release huge amount of energy and charged particles, severe events such as solar flares and Coronal mass ejections occurs(Kahler, 1992).

The huge amount of energy and charged particles released as a result of solar flares and Coronal mass ejections ionize the air molecules and cause interactions with the earth's magnetic field resulting into disturbances in the earth's magnetic fields, this disturbances are known as **geomagnetic storms**.(Schmieder, 2018).

1.2 Problem statement

The increased amount of energy and charged particles during geomagnetic storms results into heating of the ionosphere, fluctuations in the total electron content (TEC), and composition of air particularly oxygen and nitrogen as a result of ionization and

formation of new compounds. These have a great impact on the atmospheric water vapour content (the gaseous form of water that exist in the earth's atmosphere). This has got a direct impact on the refractive index (optical density of air). Since GNSS signals travel through the troposphere as wave forms, fluctuations in the refractive index results into multiple refraction thus destructive interference (or even total internal reflection in severe case) of transmitted signal hence an interruption in communication systems or even communication blackout.

Understanding the impact of geomagnetic storms on ZTD is essential for improving the accuracy of various applications that rely on precise positioning and weather forecasting.

This study aims to investigate the impact of geomagnetic storms on ZTD by analyzing a comprehensive dataset of geomagnetic storm events and corresponding ZTD measurements. By examining the relationship between these two variables, we can gain insights into the underlying mechanisms and potentially develop models to predict ZTD variations during geomagnetic storms.

The findings of this study will have practical implications for various sectors, including navigation, meteorology, and climate research. Improved understanding of the impact of geomagnetic storms on ZTD will enable more accurate positioning. It will contribute to the overall understanding of the Earth's atmosphere and its response to external disturbances, such as geomagnetic storms.

1.3 Aim

To investigate the impact of Geomagnetic Storms on zenith total delay

1.4 Objectives

To identify a Geomagnetic Storm

To determine the diurnal and seasonal variation of ZTD

To determine the ZTD during a Geomagnetic Storm.

1.6 Scope

The study utilized the statistical Dst data for 16th to 18th March, 22nd to 24th June, and 21st to 23rd December, 2015 collected by world data centre kyotto and ZTD data collected by the IGS recievers one in the magnetic crest region (MAL2) and the other in the magnetic equator regions (ADIS).

1.7 Significance

The contributed to the wealthy of knowledge in this field

The study provides mitigation models on how to mitigate the effects of geomagnetic storms on communication systems.

2.0 CHAPTER TWO: LITERATURE REVIEW

2.1 Space weather events.

The sun is continuously emitting huge amounts of energy and charged particles into the space. Various phenomena and disturbance in space are primarily driven by the sun's activities. The sudden and intense bust of radiations and particles from the surface of the sun caused by release of magnetic energy stored in the sun's atmosphere is termed as solar flare.

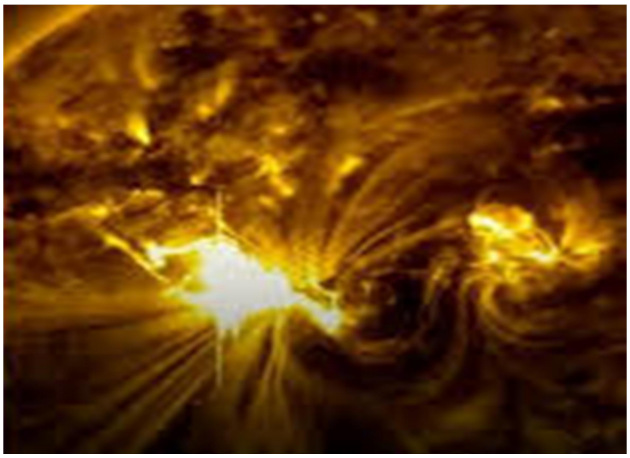

Figure 2.1. 1: Solar flares

The large scale explosion of plasma from the sun's corona is known as coronal mass ejections (CMEs). (see **figure 2.1.2)**

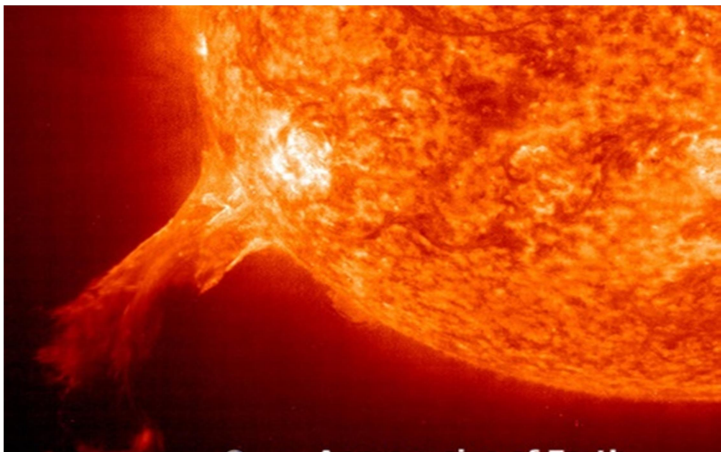

Solar flare and CMEs constitute the main severe space weather events. These events affect the Earth's atmospheric conditions and pause a big threat to the Earth's technology specifically those technologies that rely on radio wave propagation through the atmosphere.

2.2 Geomagnetic storms.

The disturbance in the Earth's magnetic fields caused due to the interaction between the earth's fields and solar activities particularly solar flares and Coronal mass ejections are termed as geomagnetic storms (Parker, 1962). These solar activities release large amounts of energy and charged particles in space and cause variations in the total electron content (TEC) in the ionosphere(Gorney, 1990). These particles ionize and react with air molecules (oxygen and nitrogen) causing fluctuations in the composition of air. This results into variation in atmospheric water vapour content. These variations in the atmospheric water vapour content causes fluctuations in the in the optical density which results in bending of radio signals which may result into interference of transmitted radio signals and may result into communication blackout in severe cases(Nikolic, Bolton, Graves, Hills, & Richer, 2013). Communication blackout may occur due to destructive interference and total internal reflection that may occur during a storm.

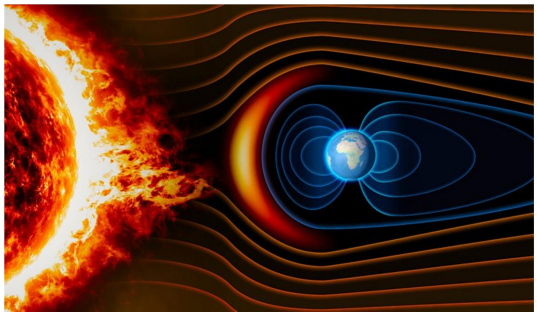

Figure 2.2. 1: Interaction of earth's field and space weather events

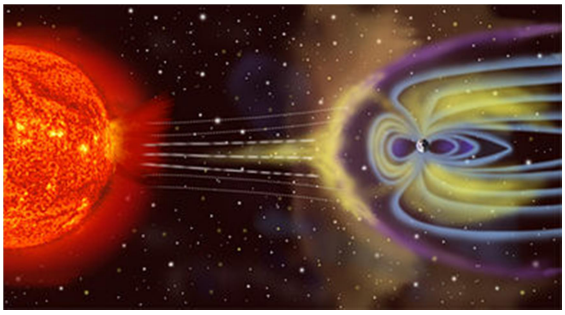

Figure 2.2. 2: Weakened earth's fields due to space weather events

2.3 Propagation of radio signals.

For any radiometric space technique, such as those utilizing GNSS, it is necessary to account for the propagation delay caused by the neutral atmosphere (Elgered & Wickert, 2017). Because of the nature of the neutral atmosphere, which is composed mainly of

gases including water vapor, radio signals are reflected or refracted when passing through the atmosphere, their speed reduces and the signals travel more slowly than the vacuum speed of light and the signals don't travel in a straight line between the signal source and the reciever. Due to these changes in speed and direction, it takes longer for the signal to reach the reciever's antenna than if they were traveling through a vacuum (Visser, 2012). This difference in time, which can also be represented in units of length, is the neutral atmosphere propagation delay. The magnitude of this delay depends on the profile of the refractive index along the signal's path, which is determined by the values of total atmospheric pressure, temperature, and the partial pressure of water vapor(Nilsson et al., 2013). The variation of these quantities at a particular location drives the variation of the delay from one day to another, over the different climate seasons. In the zenith direction, the neutral atmosphere delay at a relatively dry location at sea level is around 7.7 ns, or 2.3 m, and it increases to more than 10 m for elevation angles of about 10, and to more than 20 m at 5 (Leandro, Langley, & Santos, 2008). Typically, one does not know the actual refractive index profile at a particular location, so prediction models are often used to account for neutral atmosphere delay, particularly in real-time positioning and navigation applications

2.3 The ZTD.

The total delay experienced by a satellite signal due to the combined effects of the troposphere and ionosphere, is termed as ZTD. The ZTD is a term used in the context of Global Positioning System (GPS) and other satellite-based navigation systems to describe the delay experienced by a signal as it travels from a satellite to a receiver on the Earth's surface. This delay is caused by the signal passing through the Earth's atmosphere, which affects its speed and path. ZTD can be broken down into two main components:

Tropospheric Delay: This is the delay caused by the troposphere, the lowest layer of Earth's atmosphere. The tropospheric delay is influenced by factors such as air pressure, temperature, and humidity. It has both a dry component, which is relatively stable, and a wet component, which can vary significantly due to the amount of water vapor in the air.

Ionospheric Delay: This is the delay caused by the ionosphere, a layer of the Earth's atmosphere that contains a high concentration of ions and free electrons. The ionospheric delay is primarily influenced by the density of free electrons, which can vary with solar activity, time of day, season, and geographic location.

The total tropospheric delay in slant path delay can be mapped to the zenith direction, yielding the Zenith Tropospheric Delay (ZTD) using a mapping function depending on the elevation angle of the satellite. The ZTD is defined as the addition of the Zenith Hydrostatic Delay (ZHD) and the Zenith Wet Delay (ZHD) which are the left and the right side of Equation (1):

$$ZTD = ZHD + ZWD \quad (1)$$

$$\Delta PD = mh(E)ZHD + mw(E)ZWD \quad (2)$$

where $mh(E)$ and $mw(E)$ are the hydrostatic and wet mapping functions depending on the elevation angle. The ZTD can be determined as an integral of N in the zenith direction.

The tropospheric delay can also be separated in the hydrostatic and the wet component. That's,

$$ZTD = 10^{-6} \int_{zeni}^{direction} Nds = 10^{-6} \left\{ \int_{r}^{w} N_{dry} ds + \int_{r}^{w} N_{wet} ds \right\} \quad (3)$$

Equation (3) indicates that the Zenith Tropospheric Delay and the refractivity of the troposphere are related. Since the refractivity depends on meteorological conditions along the signal path, the ZTD can be related to these conditions. The ZTD is a parameter estimated in the Precise Point Positioning technique

3.0 CHAPTER THREE: METHODS

3.1 Identifying Geomagnetic storms

Geomagnetic storms were identified using the Dst index; a measure of geomagnetic activities. The Dst index data was collected from world data centre Kyoto for March, June and December, 2015, using website address https://www.omniweb.gsfc.nasa.gov/. The Dst data obtained was plotted and periods of Geomagnetic Storms show sharp depressions in the in the magnetic flux density.

The minimum amplitude of the Dst index was used to determine the intensity of the storm. That is, the storm is;

Moderate if the Dst lies between -50 and -100 nT

Intense if the Dst lies between -100 and -250 nT

And super-storms if the Dst ≤ -250 nT

3.2 Determination of diurnal variation of ZTD.

The daily ZTD data for March, June, and December, 2015, was obtained from existing datasets collected by the IGS recievers, one at the magnetic equator regions (ADIS) and the other at the magnetic crest regions (MAL2). Using the website address https://www.cosmic.edu/what-we-do-/suominet-weather-precipitation-data

the ZTD data obtained was plotted to obtain the diurnal variation of ZTD.

3.3 Determination ZTD variations during storm periods.

The ZTD values during identified storm periods were extracted and compared with the base line diurnal pattern. The analysis focused on detecting the deviations in the ZTD values and correlating these values with storm intensity.

4.0 CHAPTER FOUR: RESULTS AND INTERPRETATION

4.1 Identification of the storm.

Three severe Geomagnetic Storms were identified in 2015; that is;

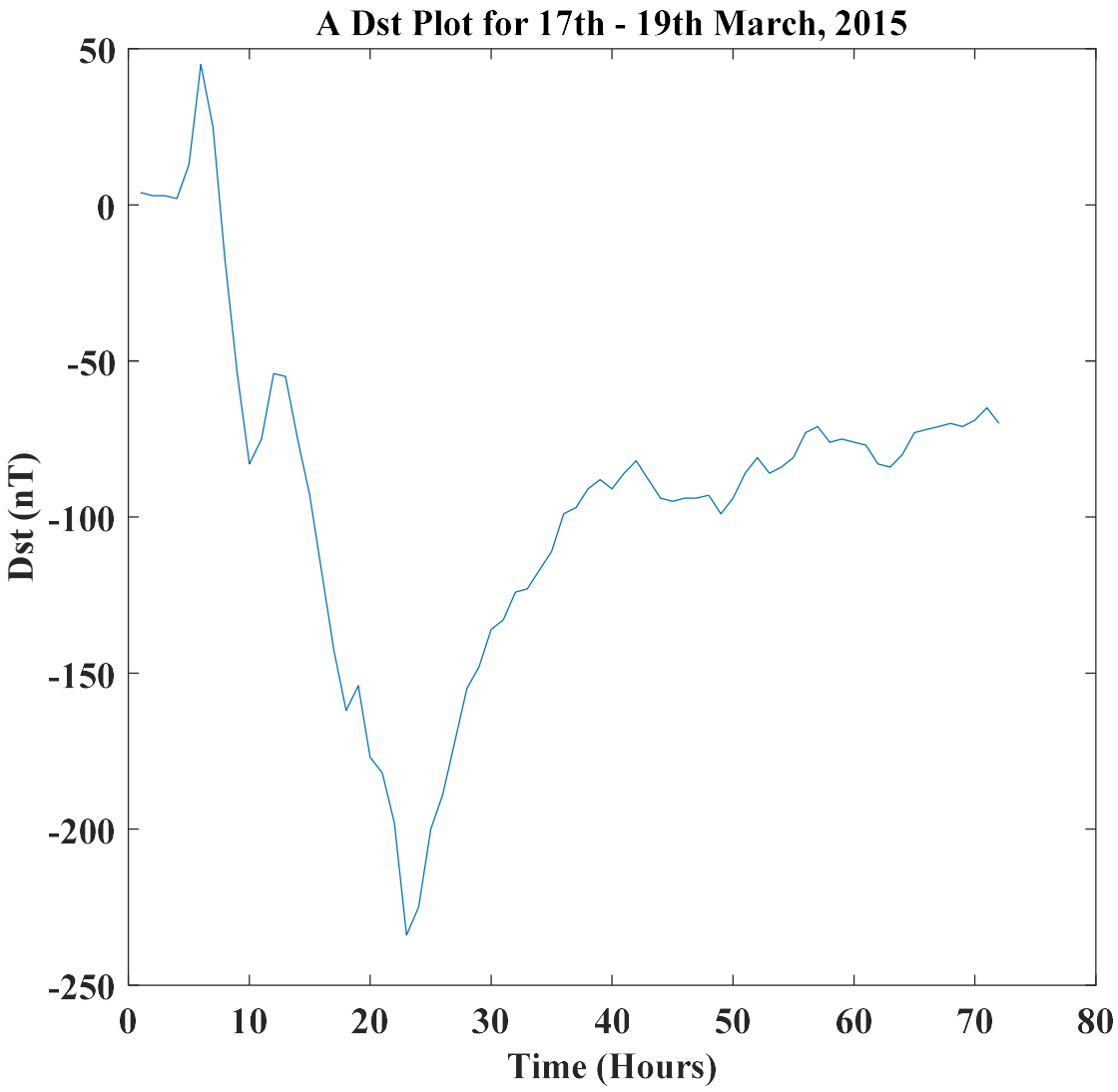

Figure 4.1. 1: A severe geomagnetic storm with a minimum Dst index of −234nT

The sudden increase in Dst values to positive values (from 3 to 13nT) shown in **Figure 4.1.1** indicated the onset of a geomagnetic storm typically associated with the initial phase of the storm, known as the storm sudden commencement (SSC). This phenomenon

was caused by the sudden compression of the Earth's magnetosphere due to an impact from a solar wind shockwave or Interplanetary Coronal Mass Ejection (ICME). When a high-speed solar wind stream or an ICME, which is a large burst of solar wind and magnetic fields rising above the solar corona, hits the Earth's magnetosphere, it causes a rapid increase in solar wind pressure. This increased pressure compresses the Earth's magnetosphere on the dayside, leading to a sudden increase in the magnetic field strength detected by ground-based magnetometers near the equator. The sudden compression resulted in a short-lived increase in the horizontal component of the magnetic field, which caused the Dst index to spike to positive values.

After this initial positive spike, the graph also show that the Dst index started to drop rapidly. The subsequent and rapid decrease in the Dst index to very big negative values less than -200nT indicates continued geomagnetic activity that led to weakening of the earth magnetic fields. This could have led to disruptions in satellite communications, power grids, and GPS systems, as well as increased auroras activity at high latitudes.

The gradual increase of the Dst index indicated that the geomagnetic activity had subsided and that the Earth's magnetosphere was returning to a more stable state. Recovery from a geomagnetic storm took several hours.

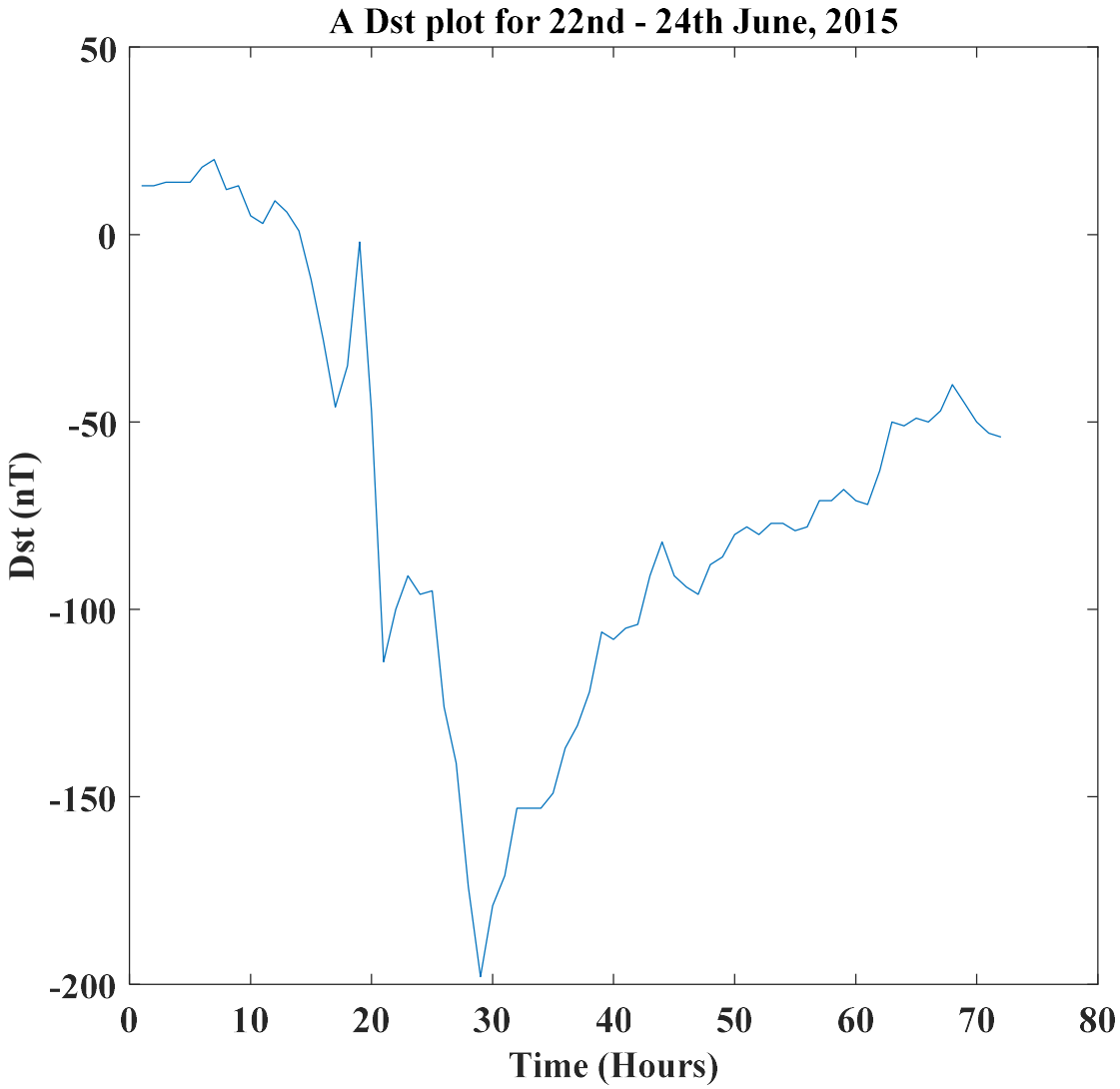

Figure 4.1. 2: A severe geomagnetic storm with a minimum Dst index of −198nT

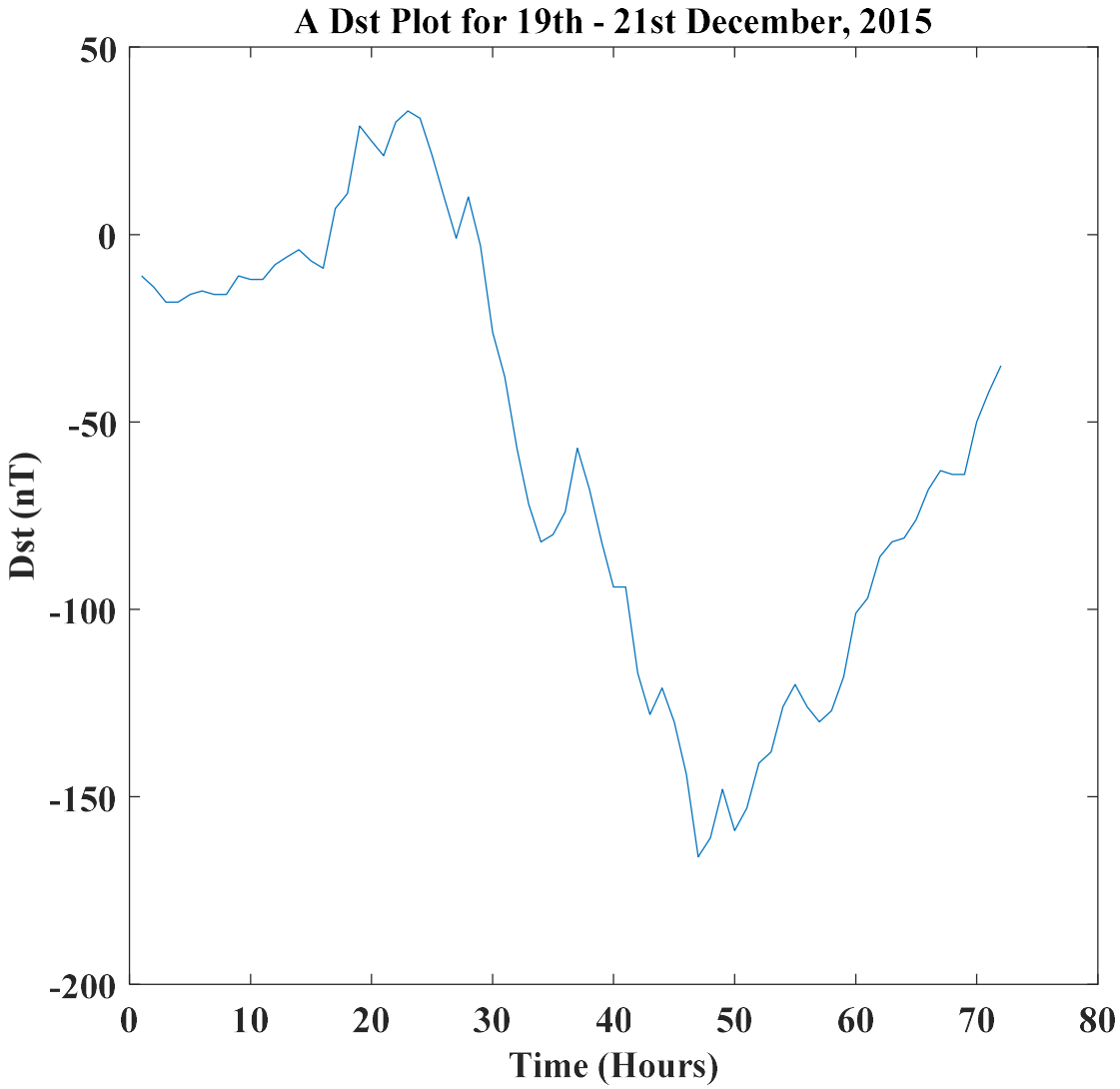

Figure 4.1. 3: A severe geomagnetic storm with a minimum Dst index of -166nT

The graph in **Figures 4.1.3** show that for a few hours the average values of the Dst index were relative stable around the origin (ranging from -4 to -11nT) indicating that there was no significant space weather event that happened during that time. The initial positive spike in Dst values at the onset of a geomagnetic storm was a result of the sudden compression of the Earth's magnetosphere by an incoming solar wind shockwave or ICME. This phase was brief and was followed sudden fall in the Dst index to large negative, indicating a significant geomagnetic disturbance. The subsequent and rapid decrease in the Dst index to very big negative values less than -150nT indicates

continued geomagnetic activity that led to weakening of the earth magnetic fields. This could have led to disruptions in satellite communications, power grids, and GPS systems, as well as increased auroras activity at high latitudes.

The gradual increase of the Dst index indicated that the geomagnetic activity had subsided and that the Earth's magnetosphere was returning to a more stable state. Recovery from a geomagnetic storm took few hours.

4.2 Diurnal variation of ZTD

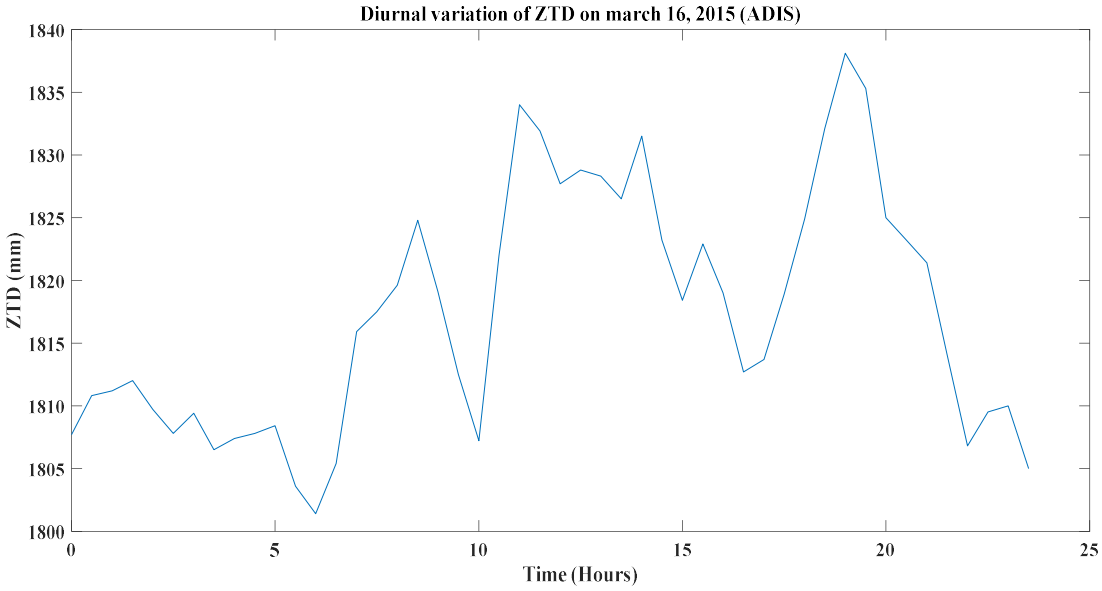

Figure 4.2. 1: Diurnal variation of ZTD for 16th March, 2015, recorded by the IGS at the magnetic equatorial region (ADIS)

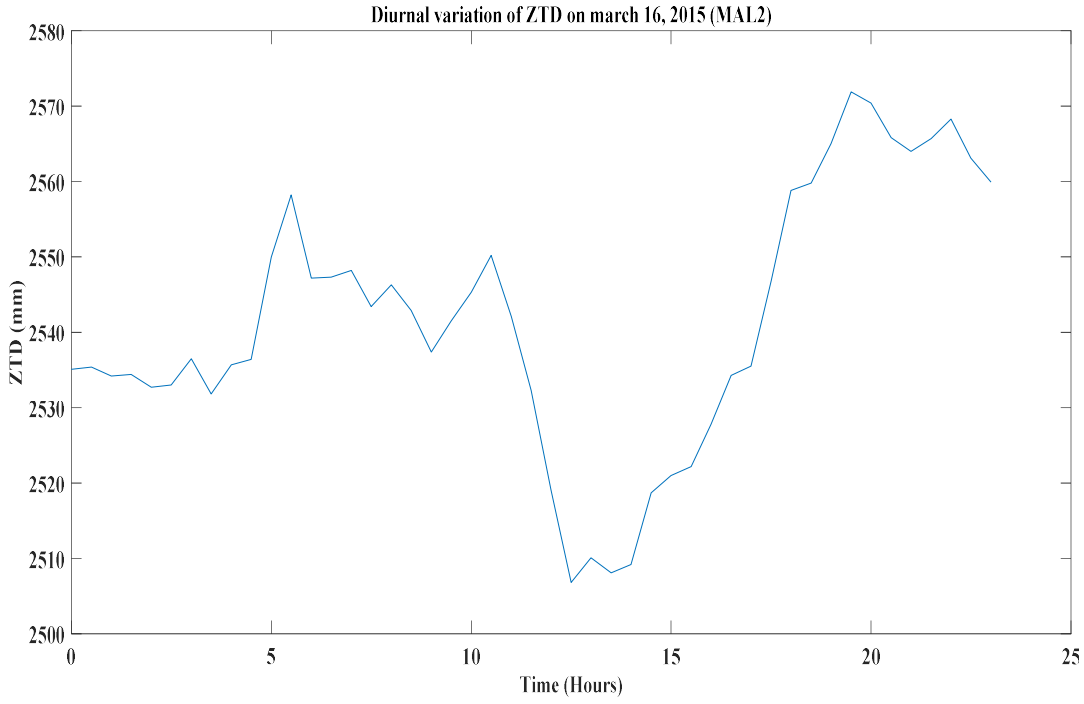

Figure 4.2. 2: Diurnal variation of ZTD on 16th March, 2015, recorded by the IGS at the magnetic crest region (MAL2)

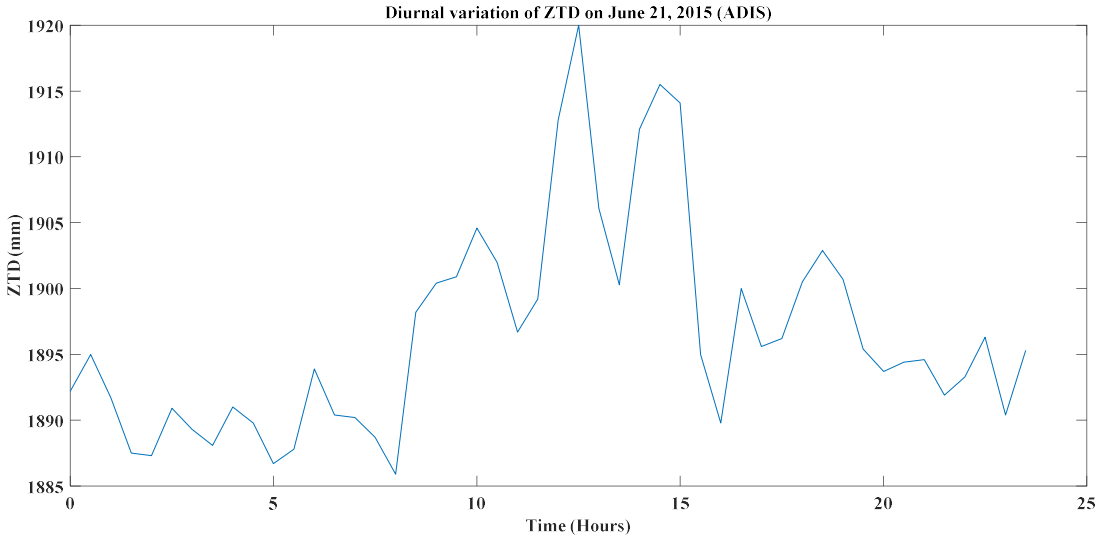

Figure 4.2. 3 Diurnal variation of ZTD on 21st June, 2015, recorded by the IGS at the magnetic equator region (ADIS)

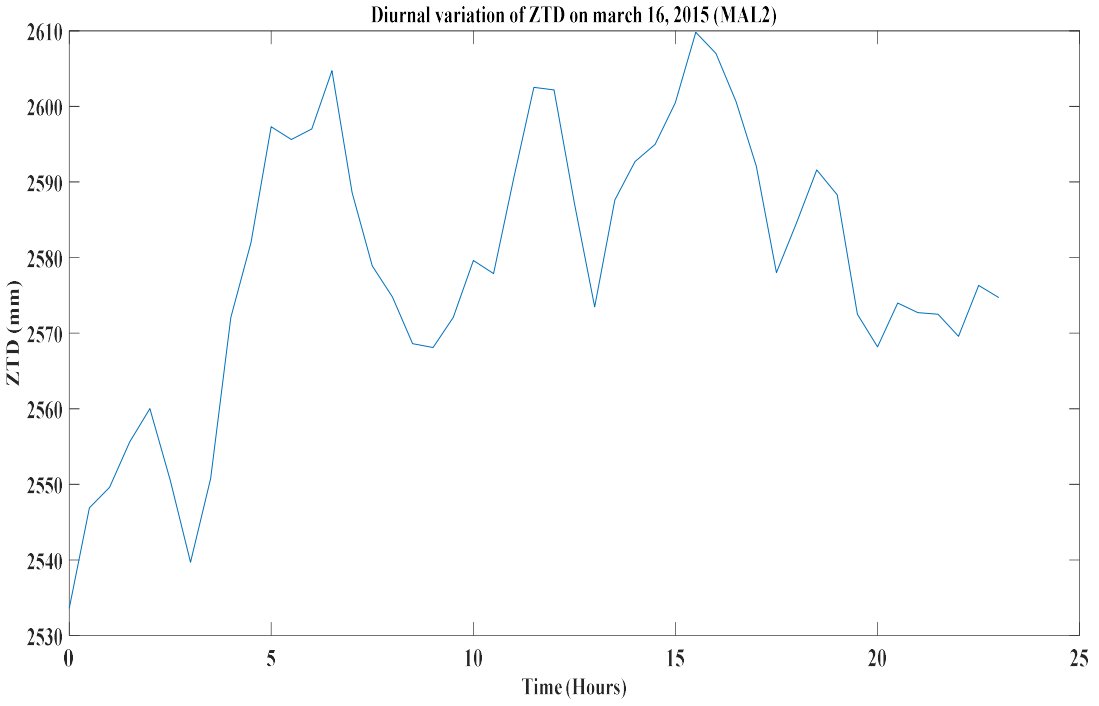

Figure 4.2. 4: Diurnal variation of ZTD on 21st June, 2015, recorded by the IGS at the magnetic crest region (MAL2)

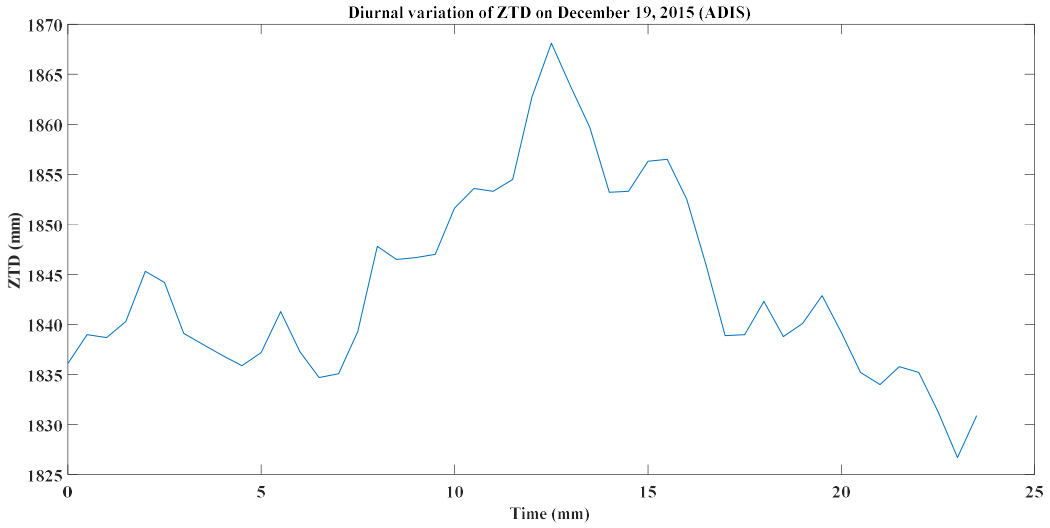

Figure 4.2. 5 Diurnal variation of ZTD for 19th December, 2015, recorded by the IGS at the magnetic equatorial region (ADIS)

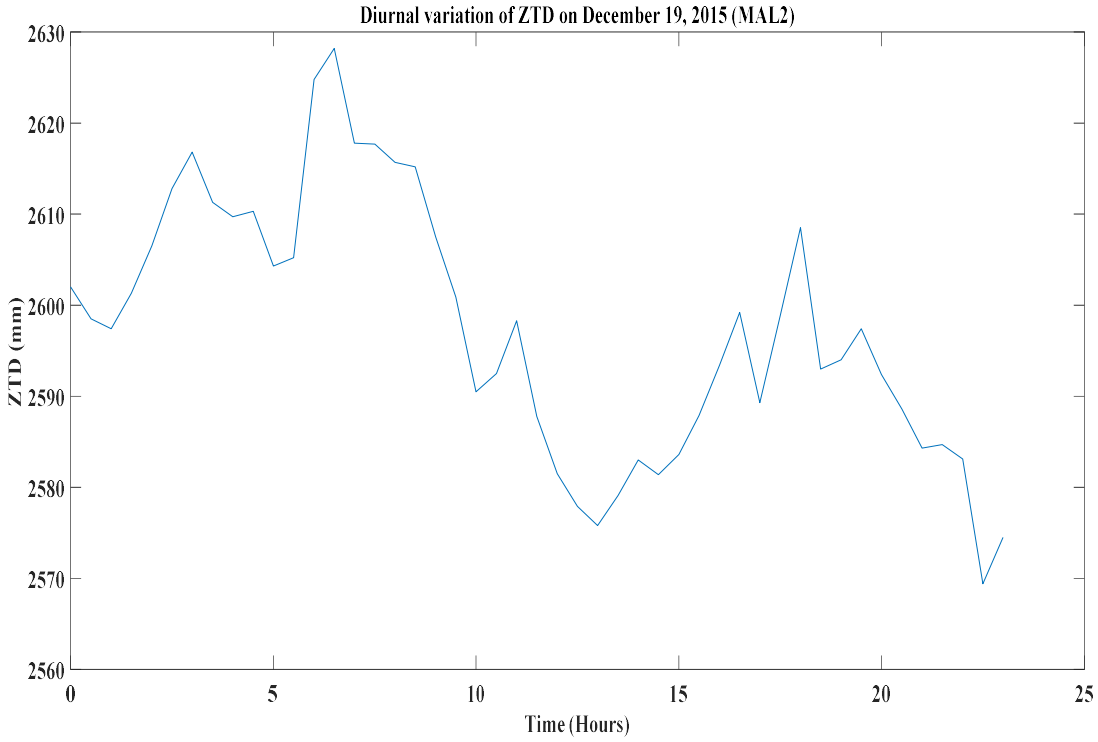

Figure 4.2. 6: Diurnal variation of ZTD on 19th Decenber, 2015, recorded by the IGS at the magnetic crest region (MAL2)

Diurnal variations exhibit a sinusoidal pattern, with ZTD values reaching peak levels during certain times of the day and dropping to minimum levels at others.

Generally, ZTD values tend to be higher during the daytime and lower during the nighttime. This is because of factors such as solar heating, atmospheric convection, and changes in the ionosphere's electron density, which influence the propagation of signals through the atmosphere. Thus, peaks in ZTD values around midday are due to the strongest solar heating, and troughs during the night are as a result of stabilized atmospheric conditions.

The magnitude of diurnal variations varies depending on factors such as geographic location, season, and local atmospheric conditions. In regions closer to the equator, where solar heating is more intense and atmospheric dynamics are more pronounced, diurnal variations in ZTD tend to be more significant compared to regions at higher latitudes.

Occasionally, sudden spikes or dips in ZTD values occur due to transient atmospheric phenomena such as passing weather systems, atmospheric disturbances, or geomagnetic activity.

4.3 Variation of ZTD during storm days

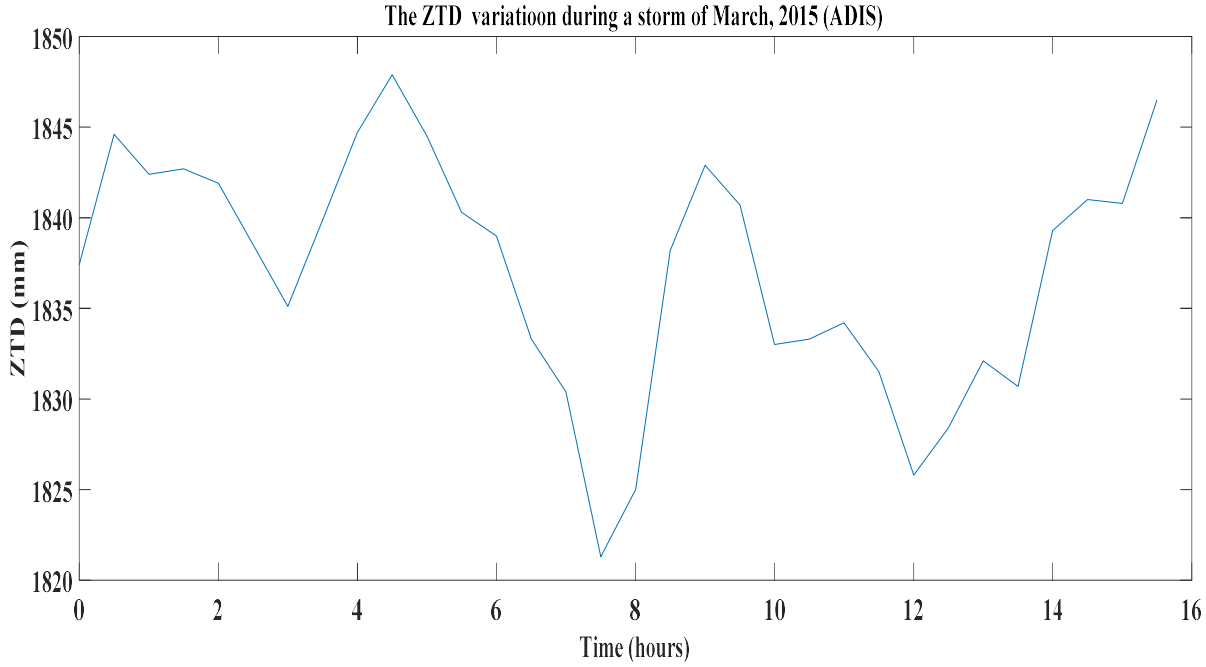

Figure 4.3. 1: variation of ZTD during storm days in March, 2015 recorded by the reciever at the magnetic equator (ADIS)

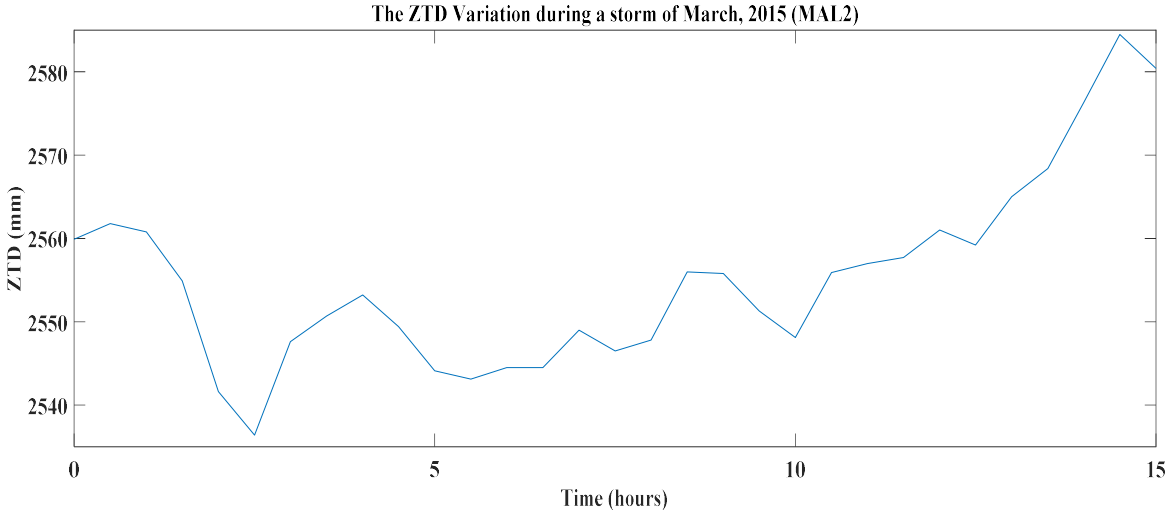

Figure 4.3. 2: Variations of ZTD during storm days of March, 2015 as recorded by the reciever in the crest region (MAL2)

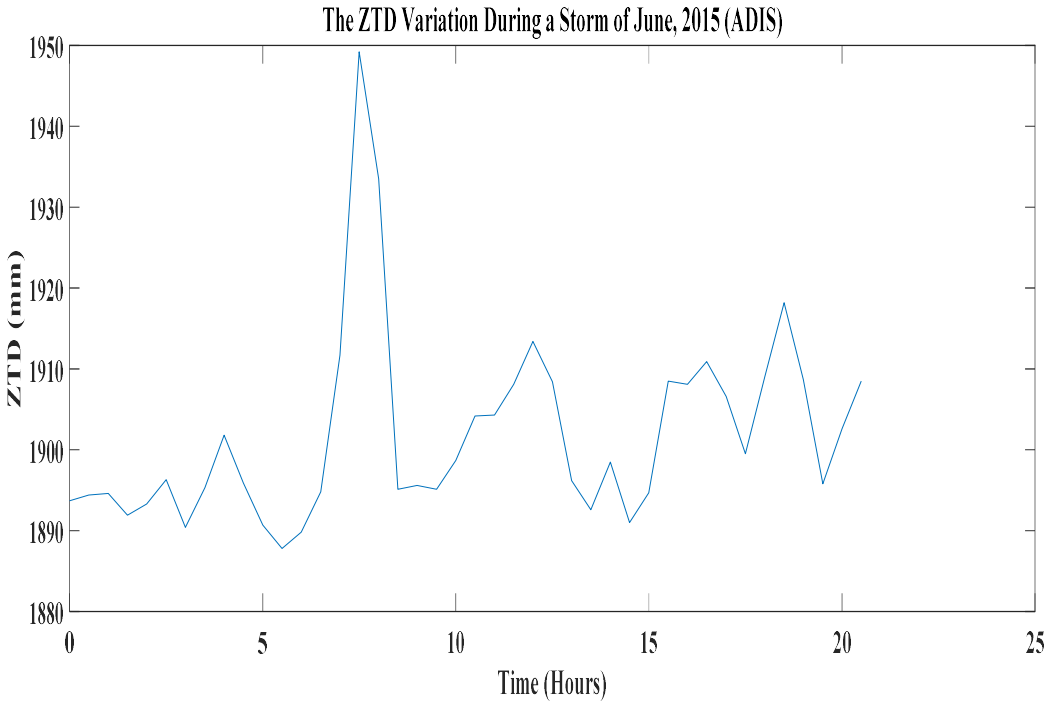

Figure 4.3. 3: Variations of ZTD during storm days of June, 2015 as recorded by the reciever at the magnetic equator (ADIS)

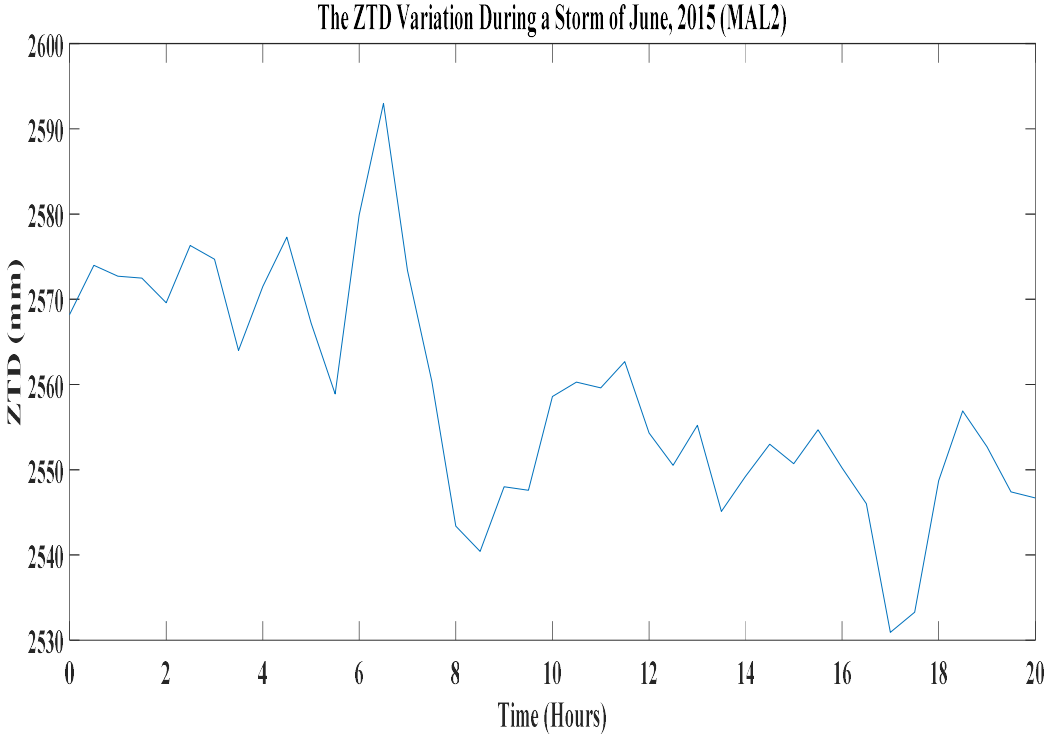

Figure 4.3. 4: Variations of ZTD during storm days of June, 2015 as recorded by the reciever in the magnetic crest region (MAL2)

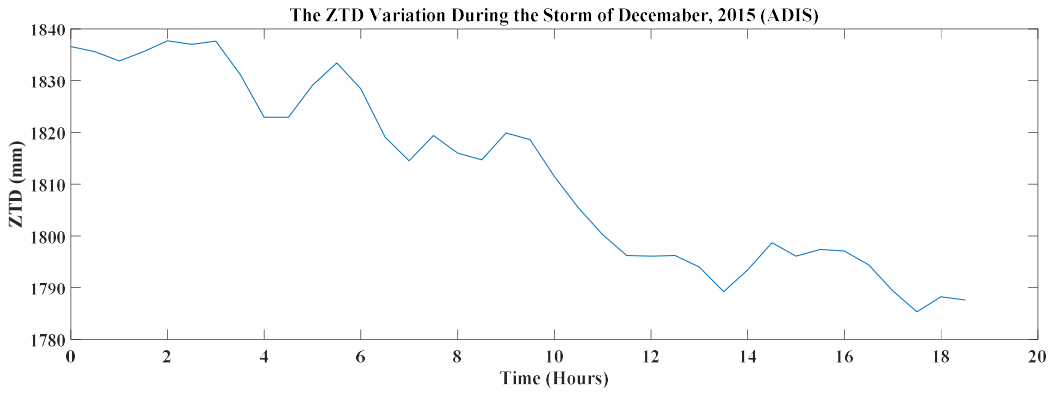

Figure 4.3. 5: Variations of ZTD during storm days of December, 2015 as recorded by the reciever at the magnetic equator (ADIS)

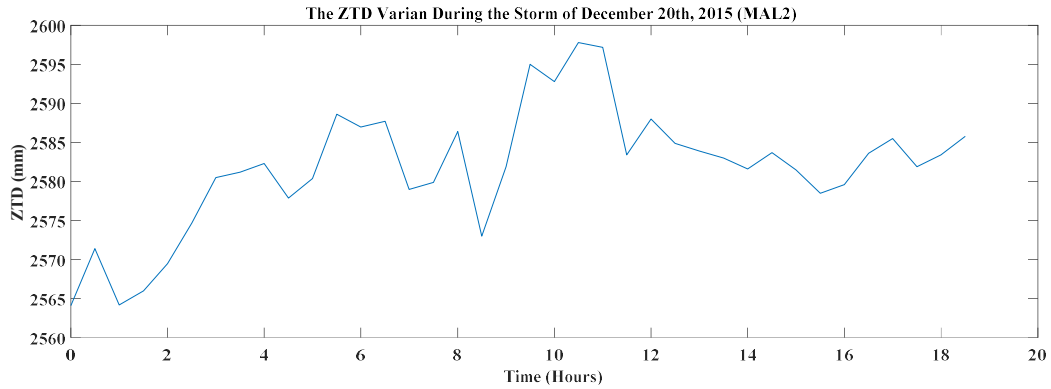

Figure 4.3. 6: Variations of ZTD during storm days of December, 2015 as recorded by the reciever in the magnetic crest region (MAL2)

During geomagnetic storm periods, the zenith total delay exhibits significant fluctuations, with a rapid increase in the zenith total delay values during the storm's main phase and gradually decreases during the recovery phase. This variation is attributed to changes in;

- The ionospheric electron density and tropospheric conditions such as increase ionospheric electron density, which in turn affects the propagation of signals from satellites to recievers on the ground. As a result, ZTD can experience rapid fluctuations during geomagnetic storms, with variations occurring over short time scales.

- SZAnd change in tropospheric water vapour content through processes like evaporation and convection, caused by geomagnetic storms. Increased water vapor content alters the refractive index of the atmosphere, affecting the speed at which electromagnetic signals propagate through it. As a result, the ZTD increases during storms due to the additional delay introduced by water vapour.

4.4 Comparison of ZTD at the magnetic equator and the magnetic crest.

The magnetic equator is the imaginary line around the Earth where the magnetic field is horizontal and its intensity is typically at its lowest. In contrast the magnetic crest, the field lines are not purely horizontal and are relatively high. These regions are typically found at higher altitude near the earth's magnetic poles.

The atmosphere's composition and density vary with location and altitude. In regions near the magnetic equator, where temperatures are generally warmer and humidity levels are higher, the atmosphere is thicker and more variable. This can result in higher ZTD values due to increased atmospheric delay caused by factors like water vapor content, temperature gradients, and pressure variations.

During a geomagnetic storm, the magnetic equator and crest are both influenced by geomagnetic activity, but their responses differ. The crest is often associated with geomagnetic disturbances, such as magnetic storms, which can cause fluctuations in the ionosphere and affect the propagation of signals through the atmosphere. These disturbances lead to variations in ZTD values, with rapid changes in delay occurring during geomagnetically active periods. In contrast, the magnetic equator may experience more stable conditions in terms of geomagnetic activity, resulting in relatively consistent ZTD values over time.

4.5 Correlation analysis

Table 4.5.1: Correlation data for average hourly ZTD value and Dst for 17th March, 2015

$ZTD(x)$	$Dst(y)$	x^2	y^2	xy
1814.7	−4.0	3293136.09	16.0	−7258.8
1822.1	−3.0	3320048.41	9.0	−5466.3
1823.1	−3.0	3323693.61	9.0	−5469.3
1829.5	−2.0	3347070.25	4.0	−3659
1833.2	−13.0	3360622.24	169.0	−23831.6
1834.0	−45.0	3363556.00	2025.0	−82530
1833.3	−25.0	3360988.89	625.0	−45832.5
1843.5	−18.0	3398492.25	324.0	−33183
1852.2	−54.0	3430644.84	2916.0	−100018.8
1838.3	−83.0	3379346.89	6889.0	−152578.9
1841.0	−75.0	3389281.00	5625.0	−138075
1842.6	−54.0	3395174.76	2916.0	−99500.4
1840.2	−55.0	3386336.04	3025.0	−101211
1837.5	−75.0	3376406.25	5625.0	−137812.5
1846.3	−93.0	3408823.69	8649.0	−171705.9
1842.4	−118.0	3394437.76	13924.0	−217403.2
1836.2	−143.0	3371630.44	20449.0	−262576.6
1825.9	−162.0	3333910.81	26244.0	−295795.8
1831.6	−154.0	3354758.56	23716.0	−282066.4
1841.8	−177.0	3392227.24	31329.0	−325998.6
1833.2	−182.0	3360622.24	33124.0	−333642.4
1832.9	−198.0	3359522.41	39204.0	−362914.2
1827.1	−234.0	3338294.41	54756.0	−427541.4
1831.4	−225.0	3354025.96	50625.0	−412065

$\sum x$	$\sum y$	$\sum x^2$	$\sum y^2$	$\sum xy$
$= 44034.0$	$= -2195.0$	$= 80793051.0$	$= 332197.0$	$= -4028136.6$

$$|r| = \left| \frac{n \sum xy - \sum x \sum y}{\sqrt{[\sum x^2 - (\sum x)^2][\sum y^2 - (\sum y)^2]}} \right|$$

$$= \left| \frac{24(-4028136.6) - (44034.0)(-2195.0)}{\sqrt{[44034.0 - (2195.0)^2][332197.0 - (-2195.0)^2]}} \right|$$

$$= |-0.9|$$

$$= 0.9$$

Table 4.5.2: Correlation data for average hourly ZTD value and Dst for 23rd June, 2015.

$ZTD(x)$	$Dst(y)$	x^2	y^2	xy
1898.9	−95.0	3605821.21	9025.0	−180395.5
1889.3	−126.0	3569454.49	15876.0	−238051.8
1892.3	−141.0	3580799.29	19881.0	−266814.3
1930.5	−174.0	3726830.25	30276.0	−335907
1914.3	−198.0	3664544.49	39204.0	−379031.4
1895.4	−179.0	3592541.16	32041.0	−339276.6
1901.5	−171.0	3615702.25	29241.0	−325156.5
1906.2	−153.0	3633598.44	23409.0	−291648.6
1910.9	−153.0	3651538.81	23409.0	−292367.7
1894.4	−153.0	3588751.36	23409.0	−289843.2
1894.8	−149.0	3590267.04	22201.0	−282325.2
1901.6	−137.0	3616082.56	18769.0	−260519.2
1909.7	−131.0	3646954.09	17161.0	−250170.7
1903.1	−122.0	3621789.61	14884.0	−232178.2
1913.7	−106.0	3662247.69	11236.0	−202852.2
1902.3	−108.0	3618745.29	11664.0	−205448.4
1905.6	−105.0	3631311.36	11025.0	−200088
1900.3	−104.0	3611140.09	10816.0	−197631.2
1895.6	−91.0	3593299.36	8281.0	−172499.6
1901.6	−82.0	3616082.56	6724.0	−155931.2
1903.3	−91.0	3622550.89	8281.0	−173200.3
1899.4	−94.0	3607720.36	8836.0	−178543.6
1888.2	−96.0	3565299.24	9216.0	−181267.2
1886.4	−88.0	3558504.96	7744.0	−166003.2
$\sum x$	$\sum y$	$\sum x^2$	$\sum y^2$	$\sum xy$
$= 45639.3$	$= -3047.0$	$= 86791576.9$	$= 412609.0$	$= -5797150.8$

$$|r| = \left| \frac{n \sum xy - \sum x \sum y}{\sqrt{[\sum x^2 - (\sum x)^2][\sum y^2 - (\sum y)^2]}} \right|$$

$$= \left| \frac{24(-5797150.8) - (45639.3)(-3047.0)}{\sqrt{[86791576.9 - (45639.3)^2][412609.0 - (-3047.0)^2]}} \right|$$

$$= |-0.8|$$

$$= 0.8$$

Table 4.5.3: Correlation data for average hourly ZTD value and Dst for 17th March, 2016.

$ZTD(x)$	$Dst(y)$	x^2	y^2	xy
1834.5	−21.0	3365390.25	441.0	−38524.5
1827.2	−10.0	3338477.12	100.0	−18271.5
1827.8	−1.0	3340670.06	1.0	−1827.75
1826.2	−10.0	3334823.82	100.0	−18261.5
1821.9	−3.0	3319319.61	9.0	−5465.7
1829.3	−26.0	3346155.56	676.0	−47560.5
1831.3	−38.0	3353659.69	1444.0	−69589.4
1843.8	−57.0	3399414.06	3249.0	−105093.8
1842.1	−72.0	3393332.41	5184.0	−132631.2
1840.0	−82.0	3385600.00	6724.0	−150880
1836.1	−80.0	3371263.21	6400.0	−146888
1834.7	−74.0	3366124.09	5476.0	−135767.8
1837.4	−57.0	3375855.02	3249.0	−104729
1834.4	−68.0	3365023.36	4624.0	−124739.2
1822.9	−82.0	3322964.41	6724.0	−149477.8
1831.3	−94.0	3353476.56	8836.0	−172137.5
1823.8	−94.0	3326064.06	8836.0	−171432.5
1817.0	−117.0	3301307.30	13689.0	−212583.2
1815.4	−128.0	3295495.62	16384.0	−232364.8
1819.3	−121.0	3309670.56	14641.0	−220129.3
1808.5	−130.0	3270491.40	16900.0	−235098.5
1798.2	−144.0	3233523.24	20736.0	−258940.8
1796.2	−166.0	3226154.82	27556.0	−298160.9
1791.6	−161.0	3209830.56	25921.0	−288447.6
$\sum x$	$\sum y$	$\sum x^2$	$\sum y^2$	$\sum xy$
$= 43790.3$	$= -1836.0$	$= 79904086.8$	$= 197900.0$	$= -3339002.6$

$$|r| = \left| \frac{n \sum xy - \sum x \sum y}{\sqrt{[\sum x^2 - (\sum x)^2][\sum y^2 - (\sum y)^2]}} \right|$$

$$= \left| \frac{24(-3339002.6) - (43790.3)(-1836.0)}{\sqrt{[79904086.8 - (43790.3)^2][197900.0 - (-1836.0)^2]}} \right|$$

$$= |-0.7|$$

$$= 0.7$$

The correlation between ZTD and Dst reveal a strong correlation ($|r| \geq 0.7$) indicating a significant relationship between the two. This suggests that geomagnetic storms have a pronounced impact on zenith total delay, leading to increased delay in of radio signals thus a significant impact on communication systems.

5.0 CHAPTER 5: CONCLUSION AND RECOMMENDATION

5.1 Conclusion

Geomagnetic storms have a significant impact on ZTD, leading to variation is signal delays and leading to increased errors in GPS positioning and navigation which causes potential disruptions in communication systems.

The diurnal variation in ZTD suggest that atmospheric conditions plays a significant on signal propagation and thus must be considered when designing and operating communication systems that rely on GPS technology.

The increased ZTD during storm periods hights the need for robust communication system that can adopt and mitigate the impact of geomagnetic and other related events.

5.2 Recommendations

1. Geomagnetic storms should be continuously monitored using a network of geomagnetic observatories and spacecraft. This can be done by developing predictive models that forecast geomagnetic storms and their potential impact on communication systems.

2. Communication systems, particularly GNSS and radio communication networks, should be designed with built-in resilience to geomagnetic storms; that's backup systems and redundant infrastructure should be implemented to ensure continuity of critical services during geomagnetic storms.

3. Communication systems should be optimized to account for ZTD variations during geomagnetic storms. System designers should consider the effects of geomagnetic storms on signal propagation and timing.

5. Further studies should focus on developing more accurate predictive models for geomagnetic storms and their impact on communication systems. Investigations into the spatial and temporal variability of ZTD during geomagnetic storms should be conducted.

References

1. Bhattacharyya, A. (2022). Equatorial plasma bubbles: A review. *Atmosphere, 13*(10), 1637.
2. Bock, O., Willis, P., Lacarra, M., & Bosser, P. (2010). An inter-comparison of zenith tropospheric delays derived from DORIS and GPS data. *Advances in Space Research, 46*(12), 1648-1660.
3. Bonafoni, S., Biondi, R., Brenot, H., & Anthes, R. (2019). Radio occultation and ground-based GNSS products for observing, understanding and predicting extreme events: A review. *Atmospheric research, 230*, 104624.
4. Elgered, G., & Wickert, J. (2017). Monitoring of the neutral atmosphere. *Springer Handbook of Global Navigation Satellite Systems*, 1109-1138.
5. Ghoddousi-Fard, R. (2023). Modelling tropospheric gradients and parameters from NWP models: Effects on GPS estimates.
6. Gorney, D. (1990). Solar cycle effects on the near-Earth space environment. *Reviews of Geophysics, 28*(3), 315-336.
7. Grinter, T., & Roberts, C. (2013). *Real time precise point positioning: are we there yet.* Paper presented at the IGNSS Symposium.
8. Guerova, G., Jones, J., Douša, J., Dick, G., de Haan, S., Pottiaux, E., . . . Vedel, H. (2016). Review of the state of the art and future prospects of the ground-based GNSS meteorology in Europe. *Atmospheric Measurement Techniques, 9*(11), 5385-5406.
9. Hernández-Pajares, M., Juan, J. M., Sanz, J., Aragón-Àngel, À., García-Rigo, A., Salazar, D., & Escudero, M. (2011). The ionosphere: effects, GPS modeling and the benefits for space geodetic techniques. *Journal of Geodesy, 85*, 887-907.
10. Horányi, M. (1996). Charged dust dynamics in the solar system. *Annual review of astronomy and astrophysics, 34*(1), 383-418.
11. Jakowski, N., Mayer, C., Wilken, V., & Hoque, M. M. (2008). Ionospheric impact on GNSS signals. *Física de la Tierra, 20*, 11.
12. Kahler, S. (1992). Solar flares and coronal mass ejections. *Annual review of astronomy and astrophysics, 30*(1), 113-141.
13. Langley, R. B. (2007). Propagation of the GPS signals. *GPS for Geodesy*, 103-140.
14. Leandro, R. F., Langley, R. B., & Santos, M. C. (2008). UNB3m_pack: a neutral atmosphere delay package for radiometric space techniques. *GPS solutions, 12*, 65-70.
15. Leckner, B. (1978). The spectral distribution of solar radiation at the earth's surface—elements of a model. *Solar energy, 20*(2), 143-150.
16. Mendez Astudillo, J., Lau, L., Tang, Y.-T., & Moore, T. (2018). Analysing the zenith tropospheric delay estimates in on-line precise point positioning (PPP) services and PPP software packages. *Sensors, 18*(2), 580.
17. Meyer, J. D., & Jin, J. (2016). Bias correction of the CCSM4 for improved regional climate modeling of the North American monsoon. *Climate Dynamics, 46*, 2961-2976.
18. Nikolic, B., Bolton, R. C., Graves, S. F., Hills, R. E., & Richer, J. S. (2013). Phase correction for ALMA with 183 GHz water vapour radiometers. *Astronomy & Astrophysics, 552*, A104.
19. Nilsson, T., Böhm, J., Wijaya, D. D., Tresch, A., Nafisi, V., & Schuh, H. (2013). Path delays in the neutral atmosphere. *Atmospheric effects in space geodesy*, 73-136.

20. Ning, T., Wang, J., Elgered, G., Dick, G., Wickert, J., Bradke, M., . . . Smale, D. (2016). The uncertainty of the atmospheric integrated water vapour estimated from GNSS observations. *Atmospheric Measurement Techniques, 9*(1), 79-92.
21. Papadimitratos, P., & Jovanovic, A. (2008). *GNSS-based positioning: Attacks and countermeasures.* Paper presented at the MILCOM 2008-2008 IEEE Military Communications Conference.
22. Parker, E. (1962). Dynamics of the geomagnetic storm. *Space Science Reviews, 1*(1), 62-99.
23. Petrie, E. J., Hernández-Pajares, M., Spalla, P., Moore, P., & King, M. A. (2011). A review of higher order ionospheric refraction effects on dual frequency GPS. *Surveys in geophysics, 32*, 197-253.
24. Qiu, C., Wang, X., Li, Z., Zhang, S., Li, H., Zhang, J., & Yuan, H. (2020). The performance of different mapping functions and gradient models in the determination of slant tropospheric delay. *Remote Sensing, 12*(1), 130.
25. Schmieder, B. (2018). Extreme solar storms based on solar magnetic field. *Journal of Atmospheric and Solar-Terrestrial Physics, 180*, 46-51.
26. Singh, D., Ghosh, J. K., & Kashyap, D. (2014). Precipitable water vapor estimation in India from GPS-derived zenith delays using radiosonde data. *Meteorology and Atmospheric Physics, 123*, 209-220.
27. Ssenyunzi, R. C., Oruru, B., D'ujanga, F. M., Realini, E., Barindelli, S., Tagliaferro, G., & van de Giesen, N. (2019). Variability and accuracy of Zenith Total Delay over the East African tropical region. *Advances in Space Research, 64*(4), 900-920.
28. Suparta, W., Alauddin, M., Ali, M., Yatim, B., & Misran, N. (2007). *Remote sensing of antarctic atmospheric water vapour using ground-based GPS meteorology.* Paper presented at the 2007 5th Student Conference on Research and Development.
29. Troller, M. R. (2004). *GPS based determination of the integrated and spatially distributed water vapor in the troposphere.* ETH Zurich,
30. Vaquero-Martínez, J., & Antón, M. (2021). Review on the role of GNSS meteorology in monitoring water vapor for atmospheric physics. *Remote Sensing, 13*(12), 2287.
31. Visser, H. J. (2012). *Antenna theory and applications*: John Wiley & Sons.
32. Younes, S. A. E. (2018). Study the Effect of New Egypt Wet Mapping Function on Space Geodetic Measurements. *American Journal of Remote Sensing, 6*(1), 29-38.